Theoretical Studies of Fundamental Pathways for Alkaline Hydrolysis of Carboxylic Acid Esters in Gas Phase

Chang-Guo Zhan,[†,‡] Donald W. Landry,[†] and Rick L. Ornstein*[,‡]

Contribution from the Department of Medicine, College of Physician & Surgeons, Columbia University, New York, New York 10032, and Pacific Northwest National Laboratory, Battelle-Northwest, Environmental Technology Division, Mailstop K2−21, Richland, Washington 99352

Received September 13, 1999. Revised Manuscript Received November 15, 1999

Abstract: Fundamental reaction pathways for the alkaline hydrolysis of carboxylic acid esters, RCOOR′, were examined through a series of first-principle calculations. The reactions of six representative esters with hydroxide ion were studied in the gas phase. A total of three competing reaction pathways were found and theoretically confirmed for each of the esters examined: bimolecular base-catalyzed acyl-oxygen cleavage ($B_{AC}2$), bimolecular base-catalyzed alkyl-oxygen cleavage ($B_{AL}2$), and carbonyl oxygen exchange with hydroxide. For the two-step $B_{AC}2$ process, this is the first theoretical study to consider the individual sub-steps of the reaction process and to consider substituent effects. For the carbonyl oxygen exchange with hydroxide and for the one-step $B_{AL}2$ process, we report here the first quantitative theoretical results for the reaction pathways and for the energy barriers. The energy barrier calculated for the second step of the $B_{AC}2$ process, that is, the decomposition of the tetrahedral intermediate, is larger in the gas phase than that of the first step, that is, the formation of the tetrahedral intermediate, for all but one of the esters examined. The exception, $CH_3COOC(CH_3)_3$, does not have an α hydrogen in the leaving group. The highest energy barrier calculated for the $B_{AC}2$ process is always lower than the barriers for the oxygen exchange and for the $B_{AL}2$ process. The difference between the barrier for the $B_{AL}2$ process and the highest barrier for the $B_{AC}2$ process is only ∼1−3 kcal/mol for the methyl esters, but becomes much larger for the others. Substitution of an α hydrogen in R′ with a methyl group considerably increases the energy barrier for the $B_{AL}2$ process, and significantly decreases the energy barrier for the second step of the $B_{AC}2$ process. The calculated substituent shifts of the energy barrier for the first step of the $B_{AC}2$ process in gas phase are in good agreement with the observed substituent shifts for the base-catalyzed hydrolysis of alkyl acetates in aqueous solution. All of the calculated results are consistent with the available experimental results and lead to a deeper understanding of previously reported gas-phase experimental observations.

Introduction

The hydrolysis of carboxylic acid esters (RCOOR′) is one of the most fundamental and thoroughly studied chemical reactions.[1−3] A variety of investigations, including heavy-atom isotope experiments and spectroscopic studies,[4−8] as well as theoretical calculations,[11−15] have provided critical insights into the mechanisms of hydrolysis. Interest in this mechanism spans chemistry and biology.[3d,16] Thus, on the basis of an understanding of base-catalyzed hydrolysis of the neurotransmitter acetylcholine, transition-state analogues were designed to inhibit acetylcholinesterase, thereby yielding a variety of insecticides.[17] Similarly, the hydrolytic degradation of cocaine is of considerable interest,[10f] and a transition-state analogue of cocaine benzoyl ester hydrolysis was designed to elicit monoclonal antibodies capable of catalyzing this reaction.[18] It is expected

[†] Columbia University.

[‡] Pacific Northwest National Laboratory.

(1) (a) Bender, M. L. *Chem. Rev.* **1960**, *60*, 53. (b) Johnson, S. L. *Adv. Phys. Org. Chem.* **1967**, *5*, 237. (c) Jencks, W. P. *Chem. Rev.* **1972**, *72*, 705.

(2) (a) Bamford, C. H.; Tipper, C. F. H. Eds. *Ester Formation and Hydrolysis*; Elsevier: Amsterdam, 1972; Vol.10. (b) Ingold, C. K. *Structure and Mechanism in Organic Chemistry*, 2nd ed.; Cornell University Press: Ithaca, New York, 1969; p 1131.

(3) (a) Jones, R. A. Y. *Physical and Mechanistic Organic Chemistry*; Cambridge University Press: Cambridge, 1979; p 227. (b) McMurry, J. *Organic Chemistry*, 2nd ed.; Cole Publishing: California, 1988. (c) Lowry, T. H.; Richardson, K. S. *Mechanism and Theory in Organic Chemistry*, 3rd ed.; Harper and Row: New York, 1987. (d) Williams, A. In *Enzyme Mechanisms*; Page, M. I., Williams, A., Eds.; Burlington: London, 1987; p 123.

(4) (a) Polanyi, M.; Szabo, A. L. *Trans Faraday Soc.* **1934**, *30*, 508. (b) Bender, M. L.; Dewey, R. S. *J. Am. Chem. Soc.* **1956**, *78*, 317. (c) Samuel, D.; Silver, B. L. *Adv. Phys. Org. Chem.* **1965**, *3*, 123.

(5) (a) Bender, M. L.; Heck, H. d'A, *J. Am. Chem. Soc.* **1967**, *89*, 1211. (b) Shain, S. A.; Kirsch, J. F. *J. Am. Chem. Soc.* **1968**, *90*, 5848. (c) Rylander, P. N.; Tarbell, D. S. *J. Am. Chem. Soc.* **1950**, *72*, 3021. (d) Fukuda, E. K.; McIver, R. T., Jr. *J. Am. Chem. Soc.* **1979**, *101*, 2498.

(6) (a) Faigle, J. F. G.; Isolani, P. C.; Riveros, J. M. *J. Am. Chem. Soc.* **1976**, *98*, 2049. (b) Takashima, K.; Riveros, J. M. *J. Am. Chem. Soc.* **1978**, *100*, 6128. (c) Johlman, C. L.; Wilkins C. L. *J. Am. Chem. Soc.* **1985**, *107*, 327. (d) Bender, M. L.; Thomas, R. J. *J. Am. Chem. Soc.* **1961**, *83*, 4189. (e) Bender, M. L.; Matsui, H.; Thomas, R. J.; Tobey, S. W. *J. Am. Chem. Soc.* **1961**, *83*, 4193. (f) Bender, M. L.; Heck, H., d'A. *Ibid.* **1967**, *89*, 1211. (g) Bender, M. L.; Ginger, R. D.; Unik, J. P. *Ibid.* **1958**, *80*, 1044. (h) O'Leary, M. H.; Marlier, J. F. *J. Am. Chem. Soc.* **1979**, *101*, 3300.

(7) Takashima, K.; Jose, S. M.; do Amaral, A. T.; Riveros, J. M. *J. Chem. Soc., Chem. Commun.* **1983**, 1255.

(8) (a) Ba−Saif, S. A.; Luthra, A. K.; Williams, A. *J. Am. Chem. Soc.* **1987**, *109*, 6362. (b) Luthra, A. K.; Ba−Saif, S. A.; Chrystiuk, E.; Williams, A. *Bull. Soc. Chim. Fr.* **1988**, 392. (c) Ba−Saif, S. A.; Luthra, A. K.; Williams, A. *J. Am. Chem. Soc.* **1989**, *111*, 2647. (d) Ba-Saif, S. A.; Waring, M. A.; Williams, A. *J. Am. Chem. Soc.* **1990**, *112*, 8115. (e) Guthrie, J. P. *J. Am. Chem. Soc.* **1991**, *113*, 3941. (f) Hengge, A. *J. Am. Chem. Soc.* **1992**, *114*, 6575. (g) Marlier, J. F. *J. Am. Chem. Soc.* **1993**, *115*, 5953.

(9) (a) Bunnett, J. F. *J. Am. Chem. Soc.* **1961**, *83*, 4978. (b) Rogers, G. A.; Bruice, T. C. *J. Am. Chem. Soc.* **1973**, *95*, 4452; **1974**, *96*, 2473; **1974**, *96*, 2481. (c) Gravitz, N.; Jencks, W. P. *J. Am. Chem. Soc.* **1974**, *96*, 489. (c) Capon, B.; Ghosh, K.; Grieve, D. M. A. *Acc. Chem. Res.* **1981**, *14*, 306. (d) McClelland, R. A.; Santry, L. J. *Acc. Chem. Res.* **1983**, *16*, 394.

10.1021/ja993311m CCC: $19.00 © 2000 American Chemical Society
Published on Web 02/04/2000

that a more complete knowledge of the mechanisms of ester hydrolysis should provide useful insights into chemical and biochemical processes.

As is well-known, ester hydrolysis involves cleavage of either the acyl-oxygen or alkyl-oxygen bond.[3c] The occurrence of acyl-oxygen or alkyl-oxygen cleavage may be determined by isotopic labeling and by stereochemical studies. Both types of cleavage are often observed, and the result is a rich array of possible reaction mechanisms. We will focus only on the most common mechanisms involving specific base-catalyzed hydrolysis, that is, hydroxide ion-catalyzed hydrolysis.[3c] The base-catalyzed hydrolysis of the majority of common alkyl esters occurs by the attack of hydroxide ion at the carbonyl carbon. This mode of hydrolysis has been designated as $B_{AC}2$ (base-catalyzed, acyl-oxygen cleavage, bimolecular),[3c] and is believed to occur by a two-step mechanism.[3] However, a concerted pathway can arise in the case of esters containing very good leaving groups (corresponding to a low pK_a value for R′OH).[8] The generally accepted two-step mechanism consists of the formation of a tetrahedral intermediate (first step), followed by decomposition of the tetrahedral intermediate to products $RCOO^- + R'OH$ (second step).[3c] The first step is usually rate-determining for the hydrolysis of alkyl esters in solution.[3c,8h] On the other hand, the results[6] obtained from experiments and theoretical analyses suggested that in the gas phase the first step proceeds spontaneously and the second step becomes rate-determining. However, the nature of the tetrahedral intermediate formed in the gas-phase hydrolysis of esters was questioned by Takashima, José, Amaral, and Riveros.[7] On the basis of their experimental observation of extremely slow isotopic oxygen exchange in the gas phase and their thermochemical estimates, they suggested that the tetrahedral species was more likely a local transition state rather than a stable intermediate.[7] Finally, another less common mode of ester hydrolysis, $B_{AL}2$ (base-catalyzed, alkyl-oxygen cleavage, bimolecular),[3c] competes with the $B_{AC}2$ mode. The $B_{AL}2$ mode, which leads to the same products as the $B_{AC}2$ process, is essentially an S_N2 substitution with a carboxylate leaving group.[3c]

The reaction pathways for the $B_{AC}2$ mode of hydrolysis of methyl acetate have been studied theoretically. Hori,[12] presuming there is no energy barrier for the first step of the hydrolysis in gas phase, studied the second step, that is, the decomposition of the tetrahedral intermediate, by performing geometry optimizations at the HF/6-31G or HF/6-31+G level of theory, followed by single-point energy evaluations at the MP2/6-31+G(d,p) level. Neglecting zero-point vibration energy correction, the potential energy barrier was 8.7 kcal/mol (from the HF calculations) or 5.8 kcal/mol (from the MP2 calculations).[12] Sherer, Turner, and Shields[13] studied the first step in the gas phase. They employed AM1 and PM3 semiempirical molecular orbital methods and ab initio HF/3-21G and HF/3-21+G procedures to optimize the geometry of the transition state and evaluate the corresponding energy barrier. Additionally, they employed Cramer and Truhlar's SM3 solvation model[19] together with the PM3 molecular orbital method to calculate the energy barrier for the first step of this hydrolysis in aqueous solution. Their computations yielded an energy barrier 19.8 kcal/mol, and they were the first to report the transition-state structure. The obtained "negative" values for the energy barrier calculated at various approximation levels for the first step in the gas phase, and the contrasting SM3 results highlighted the importance of solvent effects on the energy barrier. Earlier theoretical studies on related systems also indicated that the difference between the activation energies in gas phase and in solution is due entirely to the energy needed to desolvate hydroxide ion.[4,20] Nevertheless, Sherer, Turner, and Shields found no significant difference between the calculated transition-state structures in gas phase and in solution.[13]

The reaction pathways for the $B_{AL}2$ mode of hydrolysis have not previously been subjected to calculation. For the $B_{AC}2$ mode, despite prior studies, several important issues remain. First, a remarkable discrepancy remains unresolved between the previously reported calculated results favoring a stable tetrahedral intermediate and the conclusion of Takashima et al.[7] that their experimental work favored a local transition-state. This discrepancy implies a defect either with the theoretical calculations—perhaps an inadequately low level of theory—or with the interpretation of the experimental observations. In favor of the former defect, all of the reported geometry optimizations of relevant transition states have neglected the effects of electron correlation and polarization basis functions. Ab initio studies on other structural problems of negatively charged molecules[21] have previously indicated that without consideration of electron correlation or without inclusion of polarization functions in the employed basis set, the optimized geometries could be qualitatively incorrect. For example, the linear geometries of the C_4N^-, C_6N^-, and C_7N^- anions optimized at the HF/3-21G level are all associated with local minima on the corresponding potential-energy surfaces. However, optimizations at the MP2/6-31G(d) level or higher levels result in saddle points.[21a] Thus, the two putative transition states in the $B_{AC}2$ pathway must also be examined with sufficiently high levels of theory.

Besides, the reported "negative" energy barrier[13] should be examined further. Generally, a true transition state is associated with a first-order saddle point on the corresponding potential-energy surface. A first-order saddle point must connect with two local minima associated with a "reactant" (or an intermedi-

(10) (a) Bowden, K. *Adv. Phys. Org. Chem.* **1993**, *28*, 171. (b) Bowden, K. *Chem. Soc. Rev.* **1995**, *25*, 431. (c) Bowden, K.; Byrne, J. M. *J. Chem. Soc., Perkin Trans. 2* **1996**, 2203; **1997**, 123. (d) Bowden, K.; Izadi, J.; Powell, S. L. J. *Chem. Rev.* **1997**, 404. (e) Bowden, K.; Battah, S. *J. Chem. Soc., Perkin Trans. 2* **1998**, 1603. (f) Li, P.; Zhao, K.; Deng, S.; Landry, D. W. *Helv. Chim. Acta* **1999**, *82*, 85.

(11) (a) Dewar, M. J. S.; Storch, D. M. *J. Chem. Soc., Chem. Commun.* **1985**, *94*. (b) Dewar, M. J. S.; Storch, D. M. *J. Chem. Soc., Perkin Trans. 2* **1989**, 877.

(12) Hori, K. *J. Chem. Soc., Perkin Trans. 2* **1992**, 1629.

(13) (a) Sherer, E. C.; Turner, G. M.; Shields, G. C. *Int. J. Quantum Chem. Quantum Biol. Symp.* **1995**, *22*, 83. (b) Turner, G. M.; Sherer, E. C.; Shields, G. C. *Int. J. Quantum Chem. Quantum Biol. Symp* **1995**, *22*, 103.

(14) (a) Sherer, E. C.; Turner, G. M.; Lively, T. N.; Landry, D. W.; Shields, G. C. *J. Mol. Model.* **1996**, *2*, 62. (b) Sherer, E. C.; Yang, G.; Turner, G. M.; Shields, G. C.; Landry, D. W. *J. Phys. Chem. A* **1997**, *101*, 8526.

(15) (a) Williams, I. H.; Spangler, D.; Femec, D. A.; Maggiora, G. M.; Schowen, R. L. *J. Am. Chem. Soc.* **1980**, *102*, 6621. (b) Williams, I. H.; Maggiora, G. M.; Schowen, R. L. *J. Am. Chem. Soc.* **1980**, *102*, 7831. (c) Williams, I. H.; Spangler, D.; Femec, D. A.; Maggiora, G. M.; Schowen, R. L. *J. Am. Chem. Soc.* **1983**, *105*, 31.

(16) (a) Fersht, A. *Enzyme Structure and Mechanism*; Freeman: San Francisco, 1977. (b) Jencks, W. P. *Catalysis in Chemistry and Enzymology*; Dover Publications: New York, 1987.

(17) Ecobichon, D. J. In *Casarett & Doull's Toxicology*, 5th ed.; Klaassen, C. D., Ed.; McGraw-Hill: New York, 1996; pp 643.

(18) (a) Landry D. W.; Zhao, K.; Yang, G. X.-Q.; Glickman, M.; Georgiadis, T. M. *Science* **1993**, *259*, 1899. (b) Yang, G.; Chun, J.; Arakawa-Uramoto, H.; Wang, X.; Gawinowicz, M. A.; Zhao, K.; Landry, D. W. *J. Am. Chem. Soc.* **1996**, *118*, 5881. (c) Mets, B.; Winger, G.; Cabrera, C.; Seo, S.; Jamdar, S.; Yang, G.; Zhao, K.; Briscoe, R. J.; Almonte, R.; Woods, J. H.; Landry, D. W. *Proc. Natl. Acad. Sci. U.S.A.* **1998**, *95*, 10176.

(19) Cramer, C. J.; Truhlar, D. G. *J. Comput. Chem.* **1992**, *13*, 1089.

(20) (a) Weiner, S. J.; Singh, U. C.; Kollman, P. A. *J. Am. Chem. Soc.* **1985**, *107*, 2219. (b) Madura, J. D.; Jorgensen, W. L. *J. Am. Chem. Soc.* **1986**, *108*, 2517.

(21) (a) Zhan, C.-G.; Iwata, S. *J. Chem. Phys.* **1996**, *104*, 9058; **1996** *105*, 6578. (b) Zhan, C.-G.; Iwata, S. *J. Phys. Chem. A.* **1997**, *101*, 591. (c) Zhan, C.-G.; Iwata, S. *J. Chem. Phys.* **1997**, *107*, 7323.

ate) and a "product" (or an intermediate). Hence, a plausible calculated energy barrier can never be negative. For a bimolecular reaction, if the energy of a transition state is lower than the total energy of the separated reactants, it implies that at least one other stable structure exists between the separated reactants and the transition state.

We therefore attempt herein to establish a more complete picture of the important reaction mechanisms for hydroxide ion-catalyzed hydrolysis of esters, RCOOR′, by performing a series of first-principle quantum chemical calculations. It is expected that both substituent and solvent effects could significantly change the energy barrier associated with each transition state and the relative activation energies for different reaction pathways. In this study, we focus on the fundamental $B_{AC}2$ and $B_{AL}2$ pathways and evaluate the substituent effect by varying substituents for the carboxylic acid and alcohol moieties of the esters. We postpone to a later study the quantitative determination of the more complicated solvent effect on activation energies. For a total of six representative esters considered, we attempt to find all possible transition states and intermediates associated with the $B_{AC}2$ and $B_{AL}2$ processes as well as the carbonyl oxygen exchange with hydroxide. The calculations are compared with the available experimental results.

Calculation Methods

To determine an appropriate level of calculation for studying hydroxide ion-catalyzed reactions of esters, we carried out a series of first-principle calculations on the $B_{AC}2$ process for the hydrolysis of methyl acetate. First of all, we employed both the Hartree−Fock (HF) and the second-order Møller−Plesset (MP2) methods with various basis sets, including 6-31G, 6-31G(d), and 6-31++G(d,p), to search for and to fully optimize geometries of all possible transition states and intermediates as well as the reactants and products. In addition, the geometries optimized at the MP2/6-31++G(d,p) level were also employed to calculate energies at even higher levels, including the MP2/6-311++G(d,p), MP2/6-311++G(2d,2p), MP2/6-311++G(3d,3p), MP4SDQ/6-31++G(d,p), QCISD/6-31++G(d,p), and QCISD(T)/6-31++G(d,p). The numerical results obtained from these calculations indicate that the 6-31++G(d,p) basis set used is large enough and the MP2 method is adequate to account for the electron correlation effects. Furthermore, we tested less expensive density functional theory (DFT) calculations using Becke's three parameter hybrid exchange functional and the Lee−Yang−Parr correlation functional (B3LYP).[22] Since the results calculated at the MP2/6-31++G(d,p)//B3LYP/6-31++G(d,p) level are almost identical to those calculated at the MP2/6-31++G(d,p) level (vide infra), we chose to perform the MP2/6-31++G(d,p)//B3LYP/6-31++G(d,p) calculations on all of the systems considered in this study.

For all systems studied, vibrational frequency calculations were carried out to confirm all of the first-order saddle points and local minima on the potential-energy surfaces. Intrinsic reaction coordinate (IRC) calculations[23] were performed to verify the expected connections of the first-order saddle points with local minima on the potential-energy surfaces.

All computations reported in this study made use of Gaussian94[24] and/or Gaussian98.[25] The computations were carried out on SGI Indigo2 and Origin 200 multiprocessor computers.

Results and Discussion

Hydrolysis of Methyl Acetate. Geometry optimizations employed three different methods, HF, B3LYP and MP2, with three kinds of basis sets, 6-31G, 6-31G(d), and 6-31++G(d,p), for the reaction of methyl acetate with hydroxide ion. The optimized geometries for each species at all of the levels of theory employed are very similar and qualitatively consistent with respect to the presence of local minima or first-order saddle points on the corresponding potential-energy surfaces. The qualitative consistency of the results calculated at various levels supports the reliability of the geometry optimizations in this study.

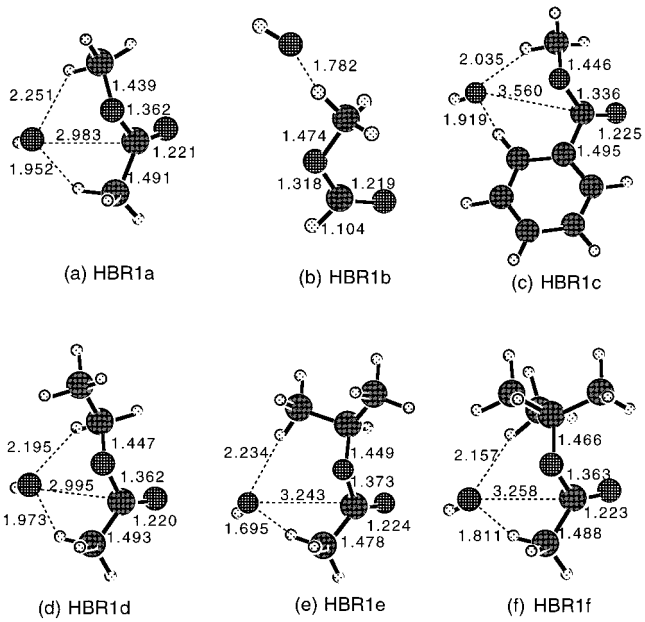

Figure 1. Geometries of the hydrogen-bonded complex HBR1 of the reactants optimized at the B3LYP/6-31++G(d,p) level.

Some important geometries optimized at the B3LYP/6-31++G(d,p) level are depicted in Figures 1 to 7. TS1a depicted in Figure 2a is the geometry of the first transition state. Note that throughout this paper the suffix "a" refers to methyl acetate, and the other letters, "b" to "f", refer to the other esters discussed later. Our consistent results qualitatively confirm the existence of the transition state found at lower approximation levels by Sherer, Turner, and Shields.[13] By performing the intrinsic reaction coordinate (IRC) procedure,[23] it is found that on the potential-energy surface this first-order saddle point connects with two local minima, one associated with a tetrahedral intermediate, INTa in Figure 3a, and the other associated with a stable hydrogen-bonded complex, HBR1a in Figure 1(a), of the reactants CH_3COOCH_3 and HO^-. As one can see from Table 1, HBR1a is ∼16−17 kcal/mol more stable than the separated reactants CH_3COOCH_3 and HO^-. Thus, the energy barrier

(22) (a) Becke, A. D., *J. Chem. Phys.* **1993**, *98*, 5648. (b) Lee, C.; Yang, W.; Parr, R. G. *Phys. Rev. B* **1988**, *37*, 785.

(23) (a) Gonzalez, C.; Schlegel, H. B. *J. Chem. Phys*. **1989**, *90*, 2154. (b) Gonzalez, C.; Schlegel, H. B. *J. Phys. Chem*. **1990**, *94*, 5523.

(24) Frisch, M. J.; Trucks, G. W.; Schlegel, H. B.; Gill, P. M. W.; B. G. Johnson, B. G.; Robb, M. A.; Cheeseman, J. R.; Keith, T.; Petersson, G. A.; Montgomery, J. A.; Raghavachari, K.; Al-Laham, M. A.; Zakrzewski, V. G.; Ortiz, J. V.; Foresman, J. B.; Cioslowski, J.; Stefanov, B. B.; Nanayakkara, A.; Challacombe, M.; Peng, C. Y.; Ayala, P. Y.; Chen, W.; Wong, M. W.; Andres, J. L.; Replogle, E. S.; Gomperts, R.; Martin, R. L.; Fox, D. J.; Binkley, J. S.; Defrees, D. J.; Baker, J.; Stewart, J. P.; Head-Gordon, M.; Gonzalez, C.; Pople, J. A. *Gaussian 94*, revision D.1; Gaussian, Inc.: Pittsburgh, PA, 1995.

(25) Frisch, M. J.; Trucks, G. W.; Schlegel, H. B.; Scuseria, G. E..; Robb, M. A.; Cheeseman, J. R.; Zakrzewski, V. G.; Montgomery, J. A.; Stratmann, R. E.; Burant, J. C.; Dapprich, S.; Millam, J. M.; Daniels, A. D.; Kudin, K. N.; Strain, M. C.; Farkas, O.; Tomasi, J.; Barone, V.; Cossi, M.; Cammi, R.; Mennucci, B.; Pomelli, C.; Adamo, C.; Clifford, S.; Ochterski, J.; Petersson, G. A.; Ayala, P. Y.; Cui, Q.; Morokuma, K.; Malick, D. K.; Rabuck, A. D.; Raghavachari, K.; Foresman, J. B.; Cioslowski, J.; Ortiz, J. V.; Stefanov, B. B.; Liu, G.; Liashenko, A.; Piskorz, P.; Komaromi, I.; Gomperts, R.; Martin, R. L.; Fox, D. J.; Keith, T.; Al-Laham, M. A.; Peng, C. Y.; Nanayakkara, A.; Gonzalez, C.; Challacombe, M.; Gill, P. M. W.; Johnson, B.; Chen, W.; Wong, M. W.; Andres, J. L.; Gonzalez, A. C.; Head-Gordon, M.; Replogle, E. S.; Pople, J. A. *Gaussian 98*, revision A.6; Gaussian, Inc.: Pittsburgh, PA, 1998.

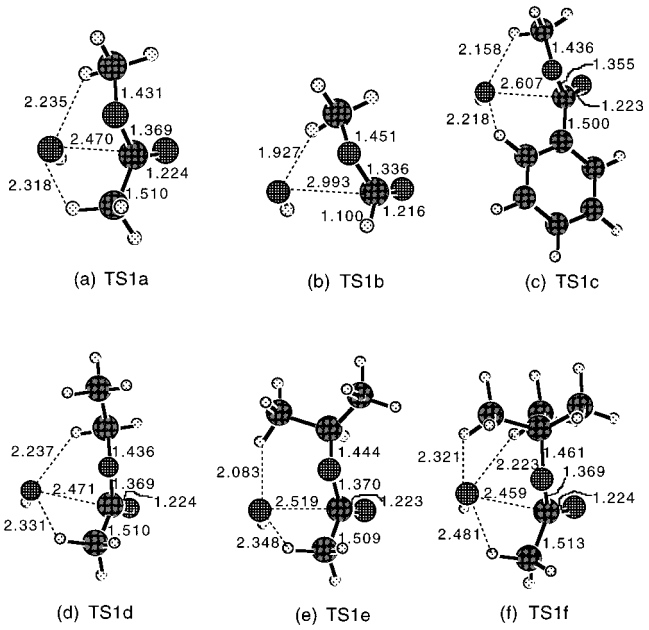

Figure 2. Geometries of the first transition state, TS1, for the $B_{AC}2$ process optimized at the B3LYP/6-31++G(d,p) level.

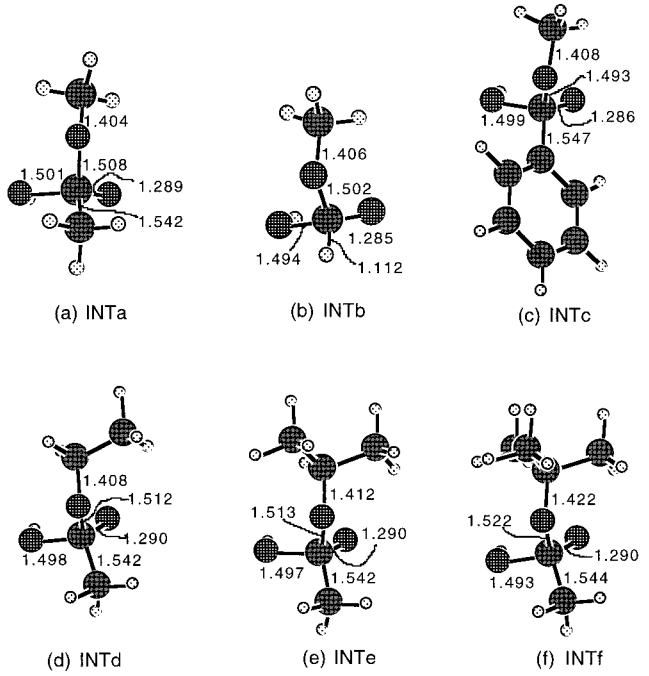

Figure 3. Geometries of the tetrahedral intermediate, INT, optimized at the B3LYP/6-31++G(d,p) level.

calculated for the formation of the tetrahedral intermediate INTa in gas phase should be the energy change from HBR1a to TS1a (a positive value), instead of that from CH_3COOCH_3 and HO^- to TS1a (a negative value).[13] TS2a depicted in Figure 4(a) is the second transition state which has also been identified as being associated with a first-order saddle point on the potential-energy surface connecting two local minima corresponding to INTa and another hydrogen-bonded complex HBPa in Table 1. In the complex HBPa, an oxygen of the product CH_3COO^- hydrogen-bonds to hydroxyl of the product CH_3OH. These results confirm those found previously on the HF/6-31G potential-energy surface by Hori.[12] We have also found another first-order saddle point associated with a transition state, TS3a in Figure 5(a), connecting with two equivalent tetrahedral intermediates, INTa in Figure 3(a) and its mirror image. The transition state structure TS3a, in which a proton stays between the two oxygen atoms, is associated with a proton transfer between the carbonyl oxygen and the hydroxide oxygen. Obviously, TS1a and INTa would be initially formed as mixtures of enantiomers and thus the significance of TS3a is not its role as a nonasymmetric species interconnecting INTa and its enantiomer. But rather, in the event of hydroxide attack with a second oxygen isotope thereby resulting in an asymmetric TS3a, this species provides a transition state for isotope exchange.

Thus, we may conclude from these results that during the gas-phase hydrolysis, when a hydroxide ion (HO^-) gradually approaches the carbonyl carbon of methyl acetate, CH_3COOCH_3 and HO^- first form the stable hydrogen-bonded complex HBR1a before progressing to the first transition state TS1a and then to the tetrahedral intermediate INTa. Furthermore, through a proton transfer from the hydroxide/hydroxyl to the ester oxygen, INTa progresses to the second transition state TS2a and then to the hydrogen-bonded complex HBPa. The decomposition of HBPa gives the separated products $CH_3COO^- + CH_3OH$, although it requires much energy in the gas phase because of the lack of solvation. Additionally, while INTa may go to HBPa through TS2a during the hydrolysis, INTa may also change into its mirror image through the transition state TS3a, thereby exchanging oxygen. It follows that there are two concurrent reaction processes, that is, the $B_{AC}2$ route of hydrolysis and the carbonyl oxygen exchange with the hydroxide. The oxygen-exchange reaction can be detected experimentally if one of the two oxygen atoms is ^{18}O labeled, and many experimental studies of $B_{AC}2$ and isotopic oxygen exchange have been reported.[5−8]

In addition to the $B_{AC}2$ and oxygen-exchange processes discussed above, we have also found another transition state, TS4a in Figure 7a, associated with the expected $B_{AL}2$ route of hydrolysis. CH_3COOCH_3 and HO^- first form a stable hydrogen-bonded complex, HBR2a in Figure 6a, before further going to the transition state TS4a and then to the same products $CH_3COO^- + CH_3OH$ as the $B_{AC}2$ route of hydrolysis.

To discuss energetics of the reactions and to quantitatively assess the convergence/accuracy of our calculated results, the detailed numerical results for the energy changes going from $CH_3COOCH_3 + HO^-$ to $CH_3COO^- + CH_3OH$ calculated for the $B_{AC}2$ route of hydrolysis at various levels are summarized in Table 1. The calculated relative energies are reported in the first 17 rows of the table, and the remaining rows refer to the relative energies plus the relative ZPV energies.

Numerical results summarized in Table 1 indicate that electron correlation is not important for the optimization of geometry, but is significant for the calculation of energy. This can be seen from the small differences between the MP2/6-31G(d) and MP2/6-31G(d)//HF/6-31G(d) results, between the MP2/6-31++G(d,p)//MP2/6-31G(d) and MP2/6-31++G(d,p)//HF/6-31G(d) results, between the MP2/6-31++G(d,p) and MP2/6-31++G(d,p)//HF/6-31++G(d,p) results, and between the MP2/6-31++G(d,p) and MP2/6-31++G(d,p)//B3LYP/6-31++G(d,p) results. Thus, the geometry optimizations with the MP2 method are adequate. To further examine the accuracy of the MP2 energy calculation for recovering the electron correlation effects, we compared the MP2 energies with those calculated using the more accurate methods, MP4SDQ, QCISD, and QCISD(T), while holding constant the basis set and geometry. One can see from Table 1 that the results calculated with the four methods are not significantly different, indicating that the MP2 method is sufficiently accurate for consideration of electron-correlation effects. Basis set dependence was evident

Table 1. Detailed Energy Changes (in kcal/mole) Calculated at Various Levels for the Base-catalyzed Hydrolysis of Methyl Acetate via $B_{AC}2$ Route[a]

	REa ↓ HBR1a	HBR1a ↓ TS1a	TS1a ↓ INTa	INTa ↓ TS2a	TS2a ↓ HBPa	HBPa ↓ PRa
Without Zero-Point Vibration Energy Correction						
HF/6-31G	−27.4	0.6	−21.2	9.9	−39.5	20.0
HF/6-31G(d)	−24.4	0.7	−22.2	9.7	−42.8	18.1
MP2/6-31G(d)//HF/6-31G(d)	−32.2	0.2	−24.2	5.8	−33.9	22.2
MP2/6-31G(d)	−33.1	0.2	−23.5	6.2	−34.7	22.9
HF/6-31++G(d,p)	−13.2	2.2	−15.0	10.9	−43.5	15.3
B3LYP/6-31++G(d,p)	−15.8	1.2	−13.3	4.6	−35.0	17.5
MP2/6-31++G(d,p)//HF/6-31G(d)	−15.3	0.0	−15.6	7.6	−32.5	18.3
MP2/6-31++G(d,p)//MP2/6-31G(d)	−13.2	0.0	−17.2	7.9	−33.7	18.4
MP2/6-31++G(d,p)//HF/6-31++G(d,p)	−16.5	2.2	−16.6	7.6	−32.3	17.7
MP2/6-31++G(d,p)// B3LYP/6-31++G(d,p)	−16.5	0.9	−15.3	7.9	−33.2	18.3
MP2/6-31++G(d,p)	−16.8	1.0	−15.2	8.1	−33.6	18.4
MP2/6-311++G(d,p)//MP2/6-31++G(d,p)	−16.9	1.1	−15.2	7.5	−33.5	18.3
MP2/6-311++G(2d,2p)//MP2/6-31++G(d,p)	−16.4	0.8	−14.6	7.2	−33.7	18.6
MP2/6-311++G(3d,3p)//MP2/6-31++G(d,p)	−16.6	0.8	−14.2	7.2	−33.5	18.8
MP4SDQ/6-31++G(d,p)//MP2/6-31++G(d,p)	−16.7	0.9	−15.2	8.7	−34.2	17.7
QCISD/6-31++G(d,p)//MP2/6-31++G(d,p)	−16.9	0.8	−15.3	8.8	−34.2	17.7
QCISD(T)/6-31++G(d,p)//MP2/6-31++G(d,p)	−17.7	0.6	−15.4	8.0	−33.0	18.4
With Zero-Point Vibration Energy Correction						
MP2/6-31++G(d,p)// B3LYP/6-31++G(d,p)	−15.7	1.1	−13.9	6.9	−32.5	17.1
MP2/6-31++G(d,p)	−16.0	1.2	−13.8	7.1	−32.9	17.2
MP2/6-311++G(d,p)//MP2/6-31++G(d,p)	−16.2	1.3	−13.8	6.5	−32.8	17.0
MP2/6-311++G(2d,2p)//MP2/6-31++G(d,p)	−15.7	1.0	−13.3	6.2	−33.0	17.3
MP2/6-311++G(3d,3p)//MP2/6-31++G(d,p)	−15.9	1.0	−12.8	6.2	−32.8	17.5
MP4SDQ/6-31++G(d,p)//MP2/6-31++G(d,p)	−16.0	1.1	−13.8	7.7	−33.5	16.5
QCISD/6-31++G(d,p)//MP2/6-31++G(d,p)	−16.2	1.0	−13.9	7.8	−33.5	16.4
QCISD(T)/6-31++G(d,p)//MP2/6-31++G(d,p)	−16.9	0.8	−14.0	7.0	−32.3	17.2

[a] REa represents the separated reactants $CH_3COOCH_3 + HO^-$, PRa represents the separated products $CH_3COO^- + CH_3OH$, HBPa represents the hydrogen-bonded complex of products CH_3COO^- and CH_3OH, and the meanings of the others can be seen from Figures 1−7.

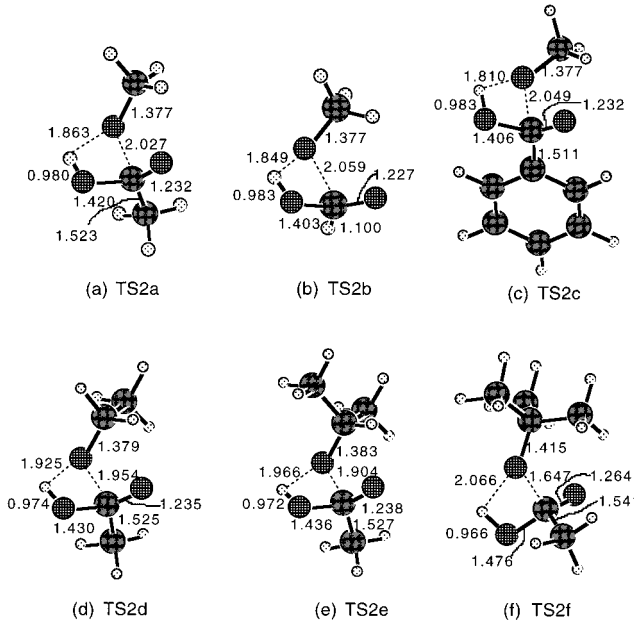

Figure 4. Geometries of the second transition state, TS2, for the $B_{AC}2$ process optimized at the B3LYP/6-31++G(d,p) level.

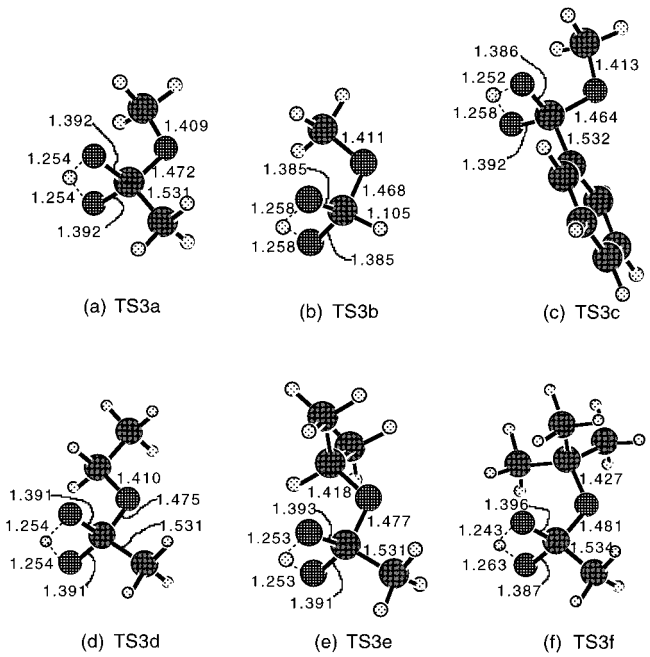

Figure 5. Geometries of the transition state, TS3, for the proton exchange between the carbonyl and the hydroxide optimized at the B3LYP/6-31++G(d,p) level.

in the significant differences in results calculated with the 6-31G(d) basis set compared to those with the 6-31++G(d,p) basis set. However, the energy calculations with larger basis sets do not significantly change the results. For example, the first energy barrier for the $B_{AC}2$ process is evaluated as 1.2 kcal/mol with the MP2/6-31++G(d,p) calculations, 1.3 kcal/mol with the MP2/6-311++G(d,p) calculations, 1.0 kcal/mol with the MP2/6-311++G(2d,2p) calculations, and 1.0 kcal/mol with the MP2/6-311++G(3d,3p) calculations. The second energy barrier for the $B_{AC}2$ process is evaluated as 7.1 kcal/mol with the MP2/6-31++G(d,p) calculations, 6.5 kcal/mol with the MP2/6-311++G(d,p) calculation, 6.2 kcal/mol with the MP2/6-311++G(2d,2p) calculations, and 6.2 kcal/mol with the MP2/6-311++G(3d,3p) calculations. Thus, the MP2/6-31++G(d,p) level of theory is sufficiently accurate for the ester hydrolysis. Furthermore, as one can see from Tables 1 and 2, the MP2/6-31++G(d,p)//B3LYP/6-31++G(d,p) results are almost identical to the corresponding MP2/6-31++G(d,p) results, especially for

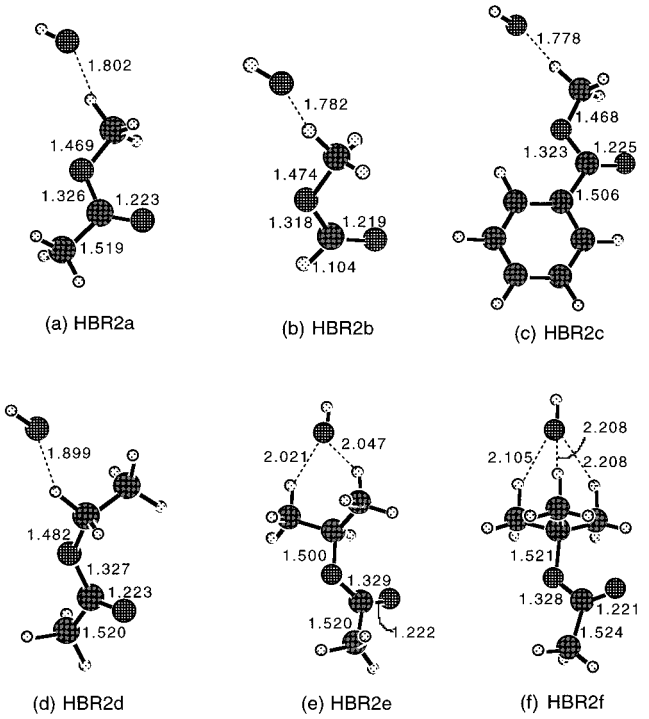

Figure 6. Geometries of the hydrogen-bonded complex HBR2 of the reactants optimized at the B3LYP/6-31++G(d,p) level.

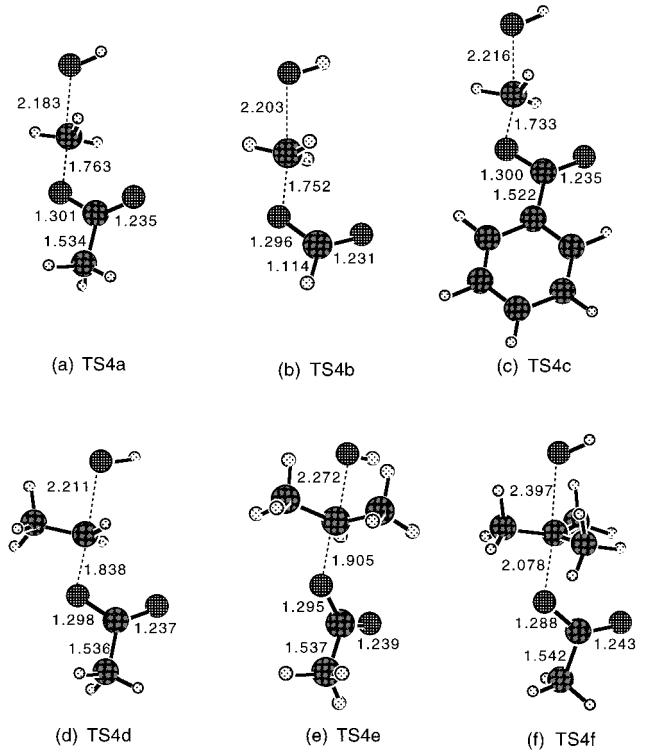

Figure 7. Geometries of the transition state, TS4, for the $B_{AL}2$ process optimized at the B3LYP/6-31++G(d,p) level.

the calculated energy barriers. The largest deviation of the energy barriers calculated at the MP2/6-31++G(d,p)//B3LYP/6-31++G(d,p) level from the corresponding barriers calculated at the MP2/6-31++G(d,p) level is 0.2 kcal/mol. This can be confirmed further by comparing the two kinds of results listed in Table 2 for methyl formate (see below). Thus, a B3LYP/6-31++G(d,p) geometry optimization followed by an MP2/6-31++G(d,p) single point energy calculation is adequate for the calculations of the other esters considered in this study.

As seen from the calculated energy barriers summarized in Table 2 and depicted in Figure 8, the barriers calculated for the first step of the $B_{AC}2$ process, that is, the formation of the tetrahedral intermediate INTa from HBR1a, and for the second step, that is, the decomposition of INTa to HBPa, are ~1 and ~7 kcal/mol, respectively. For oxygen exchange, the barriers calculated for the second step, that is, the proton exchange in the tetrahedral intermediate, and the third step, that is, the change from the mirror image of INTa to the oxygen-exchanged methyl acetate and hydroxide, are ~17 and ~14 kcal/mol, respectively. The energy barrier calculated for the one-step $B_{AL}2$ process is ~10 kcal/mol. Thus, the formation of the tetrahedral intermediate INTa should be much faster than its decomposition, and the decomposition of INTa to the products should be the rate-determining step of the $B_{AC}2$ process of the gas-phase hydrolysis. The $B_{AC}2$ process should be faster than the $B_{AL}2$ process, but the $B_{AL}2$ process should not be negligible because its energy barrier is only ~3 kcal/mol higher. The energy barriers calculated for the last two steps of the carbonyl oxygen exchange with hydroxide are much higher, and therefore, the oxygen exchange should be negligible in the gas-phase reaction.

Hydrolysis of Other Esters. To know whether the reaction pathways found for methyl acetate exist for other alkyl esters and to explore the substituent effects on the energy barriers, we have also examined other representative alkyl esters, including $HCOOCH_3$, $C_6H_5COOCH_3$, $CH_3COOCH_2CH_3$, $CH_3COOCH(CH_3)_2$, and $CH_3COOC(CH_3)_3$. We found that all three competing routes, that is, the $B_{AC}2$, $B_{AL}2$, and the oxygen exchange, found for CH_3COOCH_3 exist for each of the esters examined. The geometries optimized at the B3LYP/6-31++G(d,p) level are depicted in Figures 1−7. The calculated energy barriers are listed in Table 2 to compare with the results calculated for CH_3COOCH_3. It should be pointed out that, besides the three most common reaction processes studied here, specific esters could also have some other types of reactions with a hydroxide ion. For example, alkyl formate could also react with a hydroxide ion as $HCOOR' + HO^- \rightarrow R'OHOH^- + CO$ and $HCOOR' + HO^- \rightarrow R'O^- + H_2O + CO$.[6a,b] Esters with an alkyl group containing β hydrogens could also react with hydroxide ion in a β-elimination: $RCOOCH_2CH_3 + HO^- \rightarrow RCOO^- + H_2O + CH_2CH_2$.[6b] These reactions fall outside the scope of the present study.

As seen from Figures 1−7, with respect to each reaction step, the transition state structures optimized for different esters are generally similar to each other—although there are some minor individual differences. A notable difference exists in the first step of the $B_{AC}2$ process. The hydroxide oxygen weakly hydrogen-bonds to the alkyl groups on both sides of the carbonyl in the TS1 structures depicted in Figure 2 and in the HBR1 structures depicted in Figure 1, with the exception of TS1b and HBR1b in which $HCOOCH_3$ has only one available alkyl group. Consequently, the energy barrier calculated for the first step of the $B_{AC}2$ process of $HCOOCH_3$ is ~2 kcal/mol higher than that of the other methyl esters. In addition, while the HBR1 and HBR2 structures are different for the other esters, HBR1b and HBR2b for $HCOOCH_3$ are actually the same hydrogen-bonded species (compare Figures 1 and 6).

One can see from Table 2 that the energy barriers calculated for the $B_{AC}2$ process are all lower than the barriers for the other two processes. The difference between the barrier for the $B_{AL}2$ process and the highest barrier for the $B_{AC}2$ process is only ~1−3 kcal/mol for the methyl esters, but becomes much larger for the others. These results are consistent with the gas-phase experiments reported by Faigle, Isolani, and Riveros and by

Table 2. Energy Barriers (in kcal/mole) Calculated at the MP2/6-31++G(d,p)//B3LYP/6-31++G(d,p) Level[a] for the Base-Catalyzed Reactions of Six Esters[b]

		hydrolysis via $B_{AC}2$		oxygen exchange			hydrolysis via $B_{AL}2$
	ester	step 1	step 2	step 1	step 2	step 3	step 1
a	CH_3COOCH_3	1.1	6.9	1.1	17.0	13.9	9.8
		(1.2)	(7.1)	(1.2)	(17.1)	(13.8)	(9.8)
b	$HCOOCH_3$	3.5	6.2	3.5	18.9	15.7	8.6
		(3.4)	(6.3)	(3.4)	(18.9)	(15.5)	(8.8)
c	$C_6H_5COOCH_3$	1.5	7.0	1.5	19.3	14.6	8.0
d	$CH_3COOCH_2CH_3$	1.1	4.8	1.1	18.4	13.2	12.6
e	$CH_3COOCH(CH_3)_2$	1.5	4.3	1.5	18.4	13.2	17.4
f	$CH_3COOC(CH_3)_3$	4.4	2.5	4.4	19.8	13.6	26.3

[a] ZPV energies are included. Values in parentheses are the results calculated at the MP2/6-31++G(d,p) level. [b] The energy barriers for steps 1 and 2 of the $B_{AC}2$ process are the energy changes from HBR1 to TS1 and from INT to TS2, respectively. The energy barriers for the steps 1, 2, and 3 of the concurrent oxygen-exchange reaction are the energy changes from HBR1 to TS1, from INT to TS3, and from the mirror image of INT to the mirror image of TS1, respectively. The energy barrier for the one-step $B_{AL}2$ process is the energy change from HBR2 to TS4.

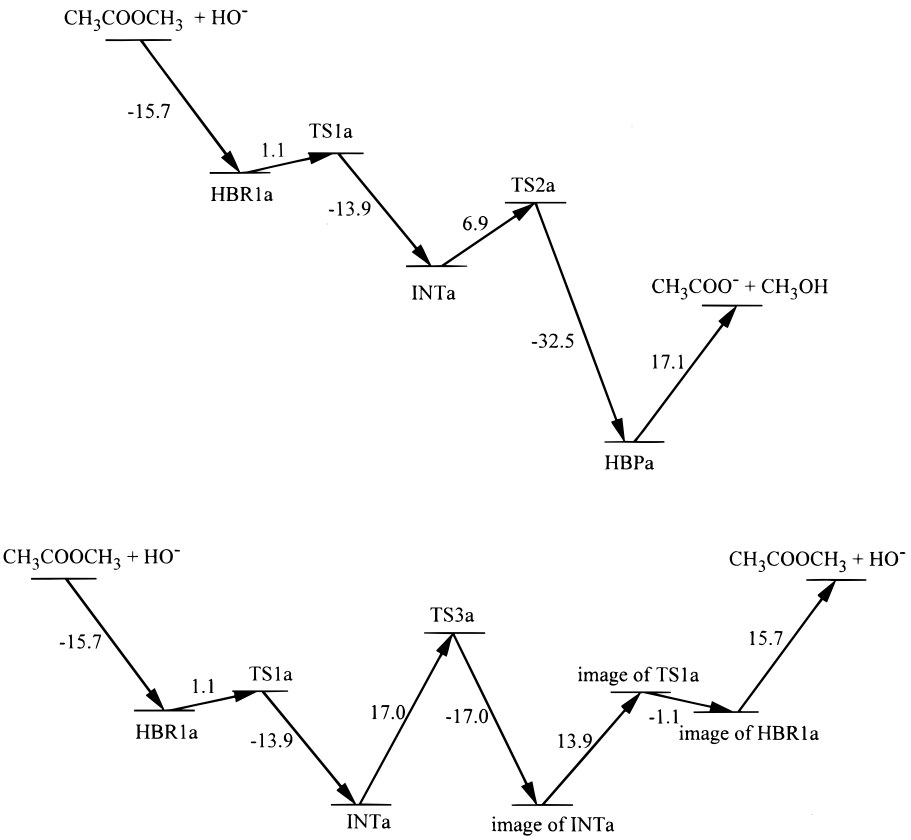

Figure 8. Energy profiles (in kcal/mole) from the MP2/6-31++G(d,p)//B3LYP/6-31++G(d,p) calculations for the concurrent $B_{AC}2$ process and the carbonyl oxygen exchange of methyl acetate with hydroxide ion.

Takashima and Riveros,[6a,b] who employed ion cyclotron resonance techniques to determine the relative rates of different reactions of ester with a hydroxide ion. Two of our examined esters, $HCOOCH_3$ and $C_6H_5COOCH_3$, were studied in their experiments. Their experimental results indicate that for $HCOOCH_3$ and $C_6H_5COOCH_3$, both the $B_{AC}2$ and $B_{AL}2$ routes are significant, and the relative contribution of the $B_{AL}2$ mechanism was ~8−27%.

The energy barriers calculated for the last two steps of the carbonyl oxygen exchange with hydroxide are all much higher than the corresponding barriers calculated for the $B_{AC}2$ process. It follows that oxygen exchange is negligible for the reactions of all six esters with hydroxide ion, which qualitatively explains why the oxygen exchange was not found in the reported gas-phase experiment.[7]

The energy barrier calculated for the $B_{AL}2$ process is significantly affected by the change of group R′. Substitution of the α hydrogen in OR′ with a methyl group considerably increases the energy barrier for the $B_{AL}2$ process. When R = CH_3 and when R′ = CH_3, CH_2CH_3, $CH(CH_3)_2$, and $C(CH_3)_3$, the calculated energy barriers are ~10, ~13, ~17, and ~26 kcal/mol, respectively. These results are in agreement with experiment, that is, that the $B_{AL}2$ process (i.e., the S_N2 substitution with the carboxylate leaving group) occurs only with an unhindered alkyl group in the alcohol moiety.[3c]

The energy barrier calculated for the second step of the $B_{AC}2$ process in gas phase is usually higher than that for the first step. The only exception is $CH_3COOC(CH_3)_3$ having no α hydrogen in the leaving group, for which the first energy barrier is the highest and the second energy barrier is the lowest among the six esters. The energy barrier calculated for the second step of the $B_{AC}2$ process mainly depends on the leaving group OR′. When R′ = CH_3, the calculated barrier is ~6−7 kcal/mol. Substitution of the α hydrogen in OR′ with one or more methyl

groups significantly decreases the energy barrier. When R = CH_3 and when R′ = CH_3, CH_2CH_3, $CH(CH_3)_2$, and $C(CH_3)_3$, the energy barriers calculated for this step are ~7, ~5, ~4, and ~3 kcal/mol, respectively.

The energy barrier calculated for the first step of the $B_{AC}2$ process in gas phase is usually very low. For the four alkyl acetates considered, changing the leaving group OR′ from R′ = CH_3 to R′ = CH_2CH_3 and to R′ = $CH(CH_3)_2$ does not significantly change the first energy barrier. However, changing OR′ from R′ = $CH(CH_3)_2$ to R′ = $C(CH_3)_3$ increases the first energy barrier by ~3 kcal/mol. The substituent shifts of the energy barrier calculated for the first step of the $B_{AC}2$ process in gas phase are in good agreement with the observed substituent shifts of the activation energy for the base-catalyzed hydrolysis of alkyl acetate in aqueous solution[26] where the first step, that is, the formation of the tetrahedral intermediate, is rate-determining. The experimental activation energies reported for R′ = CH_3, CH_2CH_3, $CH(CH_3)_2$ and $C(CH_3)_3$ are 12.2, 12.0, 12.2, and 14.3 kcal/mol, respectively.[26]

The Nature of the Tetrahedral Species. Concerning the discrepancy between the previously reported calculations and the conclusion regarding the nature of the tetrahedral species INT based on the experiments of Takashima et al.,[7] our optimized geometries and calculated energies coincide across several calculation levels and support the previous calculated results. Further, our results resolve the conflict by suggesting an alternative explanation for the gas-phase experiment[7] employed to conclude that the tetrahedral species is a local transition state rather than a stable intermediate. The ion cyclotron resonance techniques were used to study the isotopic oxygen exchange in the system $HC^{18}OOCH_3 + HO^-$ in gas phase.[7] Those authors expected that if the tetrahedral species is a stable intermediate, then they should simultaneously obtain two kinds of products for the hydrolysis ($HC^{18}OOCH_3 + HO^- \rightarrow HC^{18}OO^- + CH_3OH$) and for the oxygen exchange reaction ($HC^{18}OOCH_3 + HO^- \rightarrow HCOOCH_3 + H^{18}O^-$). Obviously, a tacit assumption was that in a stable tetrahedral intermediate the proton transfer between the hydroxyl oxygen and the carbonyl oxygen should be fast such that the proton could randomly attach to either of the two oxygen atoms. Our results do not support this assumption. According to our calculated results, the proton transfer between the two oxygen atoms must cross a transition state TS3b. The potential energy required to cross TS3b is ~19 kcal/mol for $HCOOCH_3$, prohibitively higher than the ~6 kcal/mol required to cross TS2b, and it is for this reason that the products of the oxygen-exchange reaction were not observed.

A final consideration is whether tunneling effects could ultimately change the relative magnitudes of the effective activation energies. It is expected that tunneling effects on the proton exchange should be prominent, and for this reason the effective activation energy should be significantly lower than the calculated energy barrier for the proton exchange. The question is whether the tunneling effects could be so large that the effective activation energy of the proton exchange is negligible comparing with the barrier for the breakdown of the tetrahedral intermediate INTb. A rough estimate of tunneling effects is provided by the Wigner expression,[27] as used recently by Arnaud, Bugaud, Vetere and Barone et al.[28] A proper use of the Wigner expression reveals that the tunneling effects lower the effective activation energy of the proton exchange between the two oxygen atoms in INTb by less than 1 kcal/mol at room temperature. Thus, the effective activation energy for the proton exchange in the tetrahedral intermediate is still expected to be much higher than the energy barrier (calculated as ~6 kcal/mol) for the decomposition of the intermediate in gas phase, although solvation effects could significantly change the energy barriers in a solution. Thus, our calculated results are completely consistent with the direct experimental results reported by Takashima et al.,[7] since their direct experimental results are that the $HC^{18}OO^-$ retained all of the ^{18}O initially present in the ester and that the oxygen exchange reaction was not detected within the dynamic range of ion cyclotron resonance spectroscopy.[7,29]

Conclusions

We have carried out a series of first-principle calculations on the most common reaction pathways of six representative alkyl esters with hydroxide ion in the gas phase. The convergence/accuracy of these calculations has been examined theoretically by comparing a variety of calculation methods using a variety of basis sets for the alkaline hydrolysis of methyl acetate. This comparison indicates that calculations performed at the MP2/6-31++G(d,p)//B3LYP/6-31++G(d,p) level of theory are sufficient to give reliable and accurate results for this reaction.

Three competing reaction pathways, that is, the two-step $B_{AC}2$ process, the one-step $B_{AL}2$ process, and the three-step oxygen exchange between the carbonyl and hydroxide, were found and theoretically confirmed for each of the esters considered. For the $B_{AC}2$ process, our results confirmed those at lower levels of theory in several previous reports, while providing new insights. Compared with previous theoretical studies of the first or second step for a particular ester, this is the first theoretical study to consider the individual sub-steps of the reaction process and to evaluate substituent effects. For the $B_{AL}2$ and the oxygen-exchange reactions, the present calculations provide the first quantitative theoretical results for the reaction pathways and for the energy barriers.

The energy barrier calculated for the second step of the $B_{AC}2$ process, that is, the decomposition of the tetrahedral intermediate to the products, is usually larger than that for the first step, that is, the formation of the tetrahedral intermediate, in gas phase for all of the esters examined, except for $CH_3COOC(CH_3)_3$ for

(26) Rylander, P. N.; Tarbell, D. S. *J. Am. Chem. Soc*. **1950**, *72*, 3021.
(27) Garrett, B. C.; Truhlar, D. G. *J. Phys. Chem*. **1979**, *83*, 1079.
(28) (a) Arnaud, R.; Bugaud, N.; Vetere, V.; Barone, V. *J. Am. Chem. Soc*. **1998**, *120*, 5733. (b) Barone, V.; Rega, N.; Bally, T.; Sastry, G. N. *J. Phys. Chem*. **1999**, *103*, 217.

(29) On the basis of these experimental results and the tacit assumption, however, those authors thought that either the tetrahedral species represents a local transition state which does not allow for oxygen randomization or that the forward reaction is strongly favoured due to its large exothermicity such that few collision complexes return to the reactants. They selected the first alternative on the basis of their estimate that the thermochemical stability of the tetrahedral species $HO(OCH_3)(OH)O^-$ was estimated from the heat of formation of the $HO(OCH_3)(OH)O\bullet$ radical and its electron affinity to be only ~1−7 kcal/mol lower than the reactant. This empirical approach was first used by Asubiojo and Brauman (Asubiojo, O. I.; Brauman, J. I. *J. Am. Chem. Soc*. **1979**, *101*, 3715) to analyze other reactions, employing the experimentally determined energy of an intermediate anion relative to the reactant to estimate the electron affinity of the neutral species corresponding to the intermediate anion. Their numerical results reported indicate that this approach considerably overestimated the electron affinity by 18.5 kcal/mol. This implies that the approach could underestimate the thermochemical stability of the intermediate by 18.5 kcal/mol for the same system if one would like to do so by using the experimental electron affinity. Assuming there is the same calculation error for the reaction system concerned here, as a simple test, the estimated energy of the tetrahedral species $HO(OCH_3)(OH)O^-$ could be ~19.5−25.5 kcal/mol lower than the reactants, which would be more reasonable. Our directly calculated energy of the tetrahedral species INTb is ~29 kcal/mol lower than the separated reactants. This indicates that INTb should be stable in gas phase, as should the intermediates (INT) of other esters examined in this study. Thus, there is no discrepancy between the calculated results and the available experimental results. The problem existed only in the interpretation of the experimental results.

which steric effects increase the barrier for the first step and decrease that of the second. Concerning the concurrent oxygen exchange between the carbonyl and hydroxide, the energy barriers calculated for the last two steps, that is, the proton exchange and the decomposition of the mirror image of the tetrahedral intermediate to RCOOR′ + HO^-, are both much higher than the corresponding barriers calculated for the second step of the $B_{AC}2$ process. The highest energy barrier calculated for the $B_{AC}2$ process is always lower than the barriers for the $B_{AL}2$ process. The difference between the barrier for the $B_{AL}2$ process and the highest barrier for the $B_{AC}2$ process is only ∼1−3 kcal/mol for the methyl esters and becomes much larger for the others. Substitution of the α hydrogen in R′ with a methyl group considerably increases the energy barrier for the $B_{AL}2$ process and significantly decreases the energy barrier for the second step of the $B_{AC}2$ process.

All of the calculated results are consistent with the available experimental results. Concerning the discrepancy between the previously reported calculations and the conclusion about the nature of the tetrahedral species INTb based on gas-phase experiments and the thermochemical estimates, our new results not only strongly support the previous calculations, but also lead to a more reasonable interpretation of the gas-phase experiments.

Acknowledgment. This work was supported by the Counter-drug Technology Assessment Center at the Office of National Drug Control Policy (D.W.L.) and the National Security Division and Laboratory Directed Research and Development Program (LDRD) at Pacific Northwest National Laboratory (RLO). Pacific Northwest National Laboratory is a multiprogram national laboratory operated for the U.S. Department of Energy by Battelle Memorial Institute under contract DE-AC06-76RLO 1830.

JA993311M